

To appear in The Astrophysical Journal Letters

Discovery of High-Frequency QPOs in Black Hole Candidate XTE J1859+226

Wei Cui¹, Chris R. Shrader^{2,3}, Carole A. Haswell⁴, and Robert I. Hynes⁵

ABSTRACT

We report the discovery of quasi-periodic oscillations (QPOs) at roughly 187 Hz and 150 Hz in the X-ray intensity of X-ray nova XTE J1859+226. The source was observed during a recent outburst with RXTE. Besides these high-frequency QPOs, we have also detected QPOs (and sometimes their harmonics) at 6–7 Hz, and significant broad-band variability at low frequencies. These properties, as well as the observed hard X-ray spectrum, make XTE J1859+226 a black hole candidate (BHC).

The detection of QPOs at two distinct frequencies $\gtrsim 100$ Hz in two observations separated by about 4 hours provide additional insights into the high-frequency QPO phenomenon in BHCs. The importance lies in the proposed interpretations which invariably involve the effects of strong gravity near a black hole. We compare our results to those of other BHCs, and discuss the impact of the observational data on the models in a global context.

Subject headings: binaries: general — relativity — stars: individual (XTE J1859+226) — stars: oscillations — X-rays: stars

1. Introduction

A new X-ray nova, designated as XTE J1859+226, was discovered by the ASM/RXTE on October 9, 1999 (Wood et al. 1999). Subsequent observations (2–60 keV) of the source with the PCA/RXTE revealed a hard X-ray spectrum roughly of power-law shape (Markwardt et al. 1999).

¹Center for Space Research, Massachusetts Institute of Technology, Cambridge, MA 02139; cui@space.mit.edu

²Laboratory for High-Energy Astrophysics, NASA/Goddard Space Flight Center, Greenbelt, MD 20771; shrader@gssc.gsfc.nasa.gov

³also Universities Space Research Association

⁴Dept of Physics and Astronomy, The Open University, Walton Hall, Milton Keynes, MK7 6AA, United Kingdom; C.A.Haswell@open.ac.uk

⁵Dept of Physics and Astronomy, University of Southampton, Southampton, SO17 1BJ, United Kingdom; rih@astro.soton.ac.uk

The source was detected up to 200 keV (McCollough & Wilson 1999; Dal Fiume et al. 1999). It is interesting to note that the hard X-ray flux of the source (as measured by the BATSE/CGRO; McCollough & Wilson 1999) began to decrease while the soft X-ray flux (as measured by the ASM) was still rising. This is remarkably similar to another X-ray nova XTE J1550-564 (Cui et al. 1999) and may be common for such objects.

Model fits to the X-ray spectrum of XTE J1859+226 implied a column density about $3\text{--}8 \times 10^{21} \text{ cm}^{-2}$ along the line of sight (Markwardt et al. 1999; Dal Fiume et al. 1999). The relatively low foreground extinction facilitated rapid optical follow-up observations. The optical counterpart (Garnavich et al. 1999), as well as the radio counterpart (Pooley & Hjellming 1999), was identified soon after the discovery. The optical spectrum of XTE J1859+226 showed characteristics typical of soft X-ray transients during an X-ray outburst (Wagner, R. M. et al. 1999; Hynes et al. 1999). The optical/UV continuum spectrum from the HST/STIS observations imply a binary period < 1 day (Hynes et al. 1999). Subsequent optical observations indeed detected a possible period of 9.15 hours (Garnavich & Quinn 2000), which are likely associated with the orbital motion.

XTE J1859+226 showed a strong quasi-periodic oscillation (QPO) in X-ray intensity during the rising phase of the outburst. The QPO was first detected at 0.45 Hz (Markwardt et al. 1999) and moved up to ~ 5.5 Hz as the outburst proceeded (Dal Fiume et al. 1999), similar to other X-ray novae (Fox & Lewin 1998; Cui et al. 1998, 1999; Dieters et al. 2000). The combination of the hard X-ray spectrum and QPOs makes XTE J1859+226 a black hole candidate (BHC). Here we report the detection of QPOs at much higher frequencies.

2. Observations

Fig. 1 shows the ASM light curve of XTE J1859+226. The outburst consists of periods of fast rise and exponential decay, which used to be considered typical for X-ray novae (Chen et al. 1997). The rise time (10%–90% peak) is roughly 5 days and the decay time (e-fold) about 23 days. The source experienced short-lived flares near the peak of the outburst, and a secondary maximum (at MJD 51515–51540) during the decay phase. The source continued to fade, following the secondary maximum, with roughly the same e-fold time. A much expanded light curve, shown in the inset, focuses around the peak of the outburst and clearly reveals short X-ray flares.

We obtained data from four pointed PCA observations of XTE J1859+226 around the time of the outburst peak (see Table 1). The first three observations consist of one satellite orbit and the fourth of two orbits. The count rate of the source varies by less than 30% between these observations and the X-ray spectrum remains roughly the same. Note that only a subset of the five detector units (a.k.a. PCUs) were turned on during the observations and the number of PCUs that were on varied.

3. Data Analysis and Results

We only used data from the high-resolution *Single-Bit* and *Event* modes. We first rebinned the *Event* data to the same resolution as the *Single-Bit* data (i.e., 2^{-13} s) and then combined both sets. For the analyses, we defined two energy bands: 2–5.9 keV (soft, from the low-energy *Single-Bit* data) and 5.9–60 keV (hard, from the combination of the high-energy *Single-Bit* data and the *Event* data). For each energy band, we performed a fast Fourier transform for every 128 s data segment of each observation. We normalized the power density spectrum (PDS) following the procedure of Leahy et al. (1983). Each PDS was then properly weighted and all the spectra co-added to obtain the average PDS for that observation in the chosen energy band. Fig. 2 shows the results for the hard band.

Below about 1 Hz, the PDS is dominated by broad-band variability. The spectrum of such noise is roughly of $1/f$ shape, although it is clearly more complicated in Obs. 3. Between 1–20 Hz, QPOs are prominent. Except for Obs. 3, where only one QPO is detected, the QPOs appear to be harmonically related, with the stronger peak being the fundamental component. There is a hint of a sub-harmonic component, especially in Obs. 1. The QPO is quite narrowly peaked but is much broader in Obs. 3. To quantify the QPO properties, we fit each PDS with an empirical model consisting of a power law (for the broad-band noise), Lorentzian functions (for the QPOs), and a constant (for Poisson noise). We limited the fit to the frequency range 0.01–20 Hz, except for Obs. 3, where we chose the 0.3–20 Hz range (since the broad-band noise is roughly of power-law shape only above 0.3 Hz; see Fig. 2). Table 2 shows the results. As expected, the two QPOs are harmonically related for observations 1, 2, and 4. The sub-harmonic component is significantly detected only in Obs. 1.

At frequencies above 20 Hz, broad but localized features are present in the PDS for observations 1, 2, and 4, but not for Obs. 3 (see the insets in Fig. 2). The features found in observations 1 and 4 are clearly QPO like, although fairly broad, and similar to the high-frequency QPOs found in GRO J1655-40 (Remillard et al. 1999a), XTE J1550-564 (Remillard et al. 1999b), and 4U 1630-47 (Remillard & Morgan 2000). Again, we fit the high-frequency portion (20–4000 Hz) of each PDS with the same empirical model as described above. Note that near 20 Hz the PDS is still significantly affected by the first harmonic of the low-frequency QPO whenever it is present, so the power-law component of the model actually mimics the high-frequency wing of the QPO harmonic. The best-fit parameters are also shown in Table 2.

A broad QPO is significantly detected at roughly 187 and 150 Hz in observations 1 and 4, respectively. The $Q (\equiv f/\Delta f)$ of the signal is small, on the order of unity. Only a broad “shoulder” ($Q \approx 0.5$) appears to be present in Obs. 2, and no feature is significantly detected in Obs. 3. In the latter case, however, the 3σ upper limit on the fractional rms amplitude is $\sim 2.7\%$ for the 187 Hz QPO and $\sim 3.1\%$ for the 150 Hz QPO, which are not very constraining due to poor statistics. To explore any energy dependence of such QPOs, we performed independent searches for a QPO in the soft and hard bands. The search in the soft band failed to yield any significant

detections. As an example, Fig. 3 shows the PDS from Obs. 1 for each band. Only after fixing the Lorentzian frequency and width to those of the QPO detected in the hard band, we obtained, from the fit, an rms amplitude of $1.0^{+0.4}_{-0.8}\%$ for the signal in the soft band. Therefore, the QPO is definitely stronger in the hard band; so is the 150 Hz QPO detected in Obs. 4.

For completeness, we also constructed an average cross power spectrum between the soft and hard bands for each observation (following a procedure similar to that described in, e.g., Cui 1999b), in order to measure possible phase lags. The results (also shown in Table 2) reveal significant *hard lag* (i.e., the X-ray emission in the hard band lags behind that in the soft band) associated with the fundamental component of the low-frequency QPO for observations 1, 2, and 4, but not for Obs. 3, while the broad-band variability shows *soft lags* in the vicinity of the QPO. The measured QPO lag (i.e., the difference between columns 4 and 5 in Table 2) is as large as ~ 0.55 radians, which corresponds to a time lag ~ 15 ms.

4. Discussion

The most important result from this work is the detection of QPOs at high frequencies ($\gtrsim 100$ Hz) in XTE J1859+226. These QPOs most probably originate from a single periodic process that varies in its period. It is remarkable that the period of the process can change on hour timescales. Our detections are corroborated by Markwardt et al. (2000), who found QPOs at ~ 174 Hz from their own observations. Very similar behavior is seen in XTE J1550-564: a QPO was first discovered at ~ 184 Hz during a giant X-ray flare near the peak of the outburst (Remillard et al. 1999b) and another was later detected at ~ 284 Hz at a much lower flux (Homan, Wijnands, & van der Klis 1999). These QPOs are, however, in sharp contrast to the high-frequency QPOs seen in microquasars, GRS 1915+105 (Morgan, Remillard, & Greiner 1997) and GRO J1655-40 (Remillard et al. 1999a), which were thought to maintain a constant frequency. This implies that there could be intrinsic physical differences underlying such QPOs in BHCs. Alternatively, the different behaviors may merely result from insufficient statistics or sporadic coverage. For XTE J1859+226, the QPOs are stronger at higher energies, in terms of their fractional rms amplitudes, which is typical of nearly all QPOs in BHCs (review by Cui 1999a).

Several models have been proposed to explain the high-frequency QPOs in BHCs, all of which invoke strong gravity near the central black hole (review by Cui, Chen, & Zhang 1998). It was first suggested that the QPOs might be associated with the Keplerian motion at the last stable orbit around Schwarzschild black holes (Morgan, Remillard, & Greiner 1997). Perhaps the motion of “blobs” or “hot spots” in an accretion disk extending all the way to the last stable orbit somehow causes the modulation of X-ray emission. However, the emissivity of the disk vanishes at the last stable orbit, due to the torque-free boundary condition, so it is perhaps more sensible to associate the QPOs with orbiting hot spots located in a region where the disk emissivity peaks. While appealing for its simplicity the model is incompatible with the spectral results (Cui, Chen, & Zhang 1998). Nowak et al. (1997) subsequently proposed that the QPOs are associated with

the oscillation modes in the accretion disk. Not only can such modes be supported by the disk, they also become trapped in the innermost portion of the disk, purely due to relativistic effects (Kato & Fukue 1980; Nowak & Wagoner 1992, 1993). Finally, Cui et al. (1998) argued that the QPOs could be due to the Lense-Thirring precession of the tilted circular orbits of blobs or hot spots at the inner edge of the accretion disk, motivated by observational evidence for the presence of rapidly rotating black holes in microquasars (Zhang, Cui, & Chen 1997).

All the models were initially proposed to explain the “constant frequency QPOs” in microquasars. Consequently, the accretion disk was assumed to extend to the last stable orbit in the models. Since the high-frequency QPOs now appear to be common among BHCs, an obvious question to ask now is whether the models can accommodate the QPOs that vary in frequency, as in the case of XTE J1550-564 and XTE J1859+226. For those models that involve Keplerian motion or Lense-Thirring precession, “variable frequency QPOs” can be explained if the inner edge of the accretion disk is allowed to move. Because the precession frequency in the Lense-Thirring model depends strongly on the radius of the orbit (roughly, $f \propto r^{-3}$), a $\sim 35\%$ change in the QPO frequency (as in the extreme case of XTE J1550-564) requires that the inner edge of the disk moves radially outward only by $\sim 15\%$. Therefore, the variable frequency QPOs would pose least serious challenges to this model. In comparison, the dependence of the Keplerian frequency on the orbital radius is not as steep; the inner edge of the disk would be required to move about twice as far in the Keplerian motion model. The problem is far more serious (if not fatal) for the disk oscillation model, because the oscillation modes tend to be fairly well localized in the accretion disk. While much improved statistics are clearly needed to ultimately establish the physical origin of the high-frequency QPOs in BHCs, it is clear that the discovery of variable frequency QPOs has begun to seriously constrain the models.

An additional similarity between XTE J1859+226 and XTE J1550-564 is the presence of a prominent and evolving QPO at a few Hz during the rising phase of the outburst. However, the QPO is almost certainly of a different physical origin for the two sources, because the phase lag associated with the fundamental component is of an *opposite* sign (cf. Cui, Zhang, & Chen 2000). While the complicated QPO lags in XTE J1550-564 are likely the same phenomenon as was first discovered in a subset of the QPOs of GRS 1915+105 (Cui 1999b), the hard QPO lag in XTE J1859+226 makes the QPO here similar to a second type of the low-frequency QPOs in XTE J1550-564, which were detected at a later stage of the outburst and also showed a sub-harmonic component (Wijnands, Homan, & van der Klis 1999). The phase lag measurement has, therefore, added new puzzles to the already very intriguing QPO phenomenology in BHCs (see Cui 1999b for a discussion of possible implications of different QPO lags on the models).

It has been argued, based on the observed dependence of QPO properties on mass accretion rate (as indicated by X-ray flux) and photon energy, that the QPOs in BHCs form a heterogeneous class of phenomena, each of which may well be produced by a different physical mechanism (Cui 1999a; Cui et al. 1998). For a given source, the QPOs are known to come and go in an unpredictable manner, and a different set of QPOs may dominate the PDS at different times (see

an extreme example offered by GRS 1915+105; Morgan, Remillard, & Greiner 1997). Here we have shown that such changes took place on time scales as short as roughly one hour in XTE J1859+226 (i.e., the time between Obs. 3 and Obs. 2 or 4). The source clearly behaved very differently during Obs. 3, both in terms of the QPOs and broad-band noise (see Fig. 2). It is interesting that the timing properties (low- and high-frequency QPOs plus broad-band variability) all seem to be correlated. A plausible model must, therefore, be able to account for such a global change.

We thank Jean Swank and Craig Markwardt for useful discussions. W. C. acknowledges financial support of NASA grants NAG5-7484 and NAG5-7990. C. A. H. and R. I. H were supported by grant F/00-180/A from the Leverhulme Trust.

REFERENCES

- Chen, W., Shrader, C. R., & Livio, M. 1997, *ApJ*, 491, 312
- Cui, W., Zhang, S. N., & Chen, W. 1998, *ApJ*, 492, L53
- Cui, W., Chen, W., & Zhang, S. N. 1998, *Proc. Third William Fairbank Meeting on The Lense-Thirring Effect*, Eds. L.-Z. Fang, & R. Ruffini, University “La Sapienza”, Rome, Italy, June 29 – July 4, 1998 (astro-ph/9811023).
- Cui, W., Zhang, S. N., Chen, W., & Swank, J. 1998, *BAAS*, 193, 2902
- Cui, W. 1999a, *Proc. ”High-Energy Processes in Accreting Black Holes”*, eds. J. Poutanen & R. Svensson, *ASP. Conf. Ser. Vol. 161*, 97 (astro-ph/9809408)
- Cui, W., Zhang, S. N., Chen, W., & Morgan, E. H. 1999, *ApJ*, 512, L43
- Cui, W. 1999b, *ApJ*, 514, L59
- Cui, W., Zhang, S. N., & Chen, W. 2000, *ApJ*, 531, L45
- Dal Fiume, D., et al. 1999, *IAU Circ.* 7291
- Dieters, S. W., et al. 2000, *ApJ*, in press
- Fox, D., & Lewin, W. H. G. 1998, *IAU Circ.* 6964
- Garnavich, P. M., Stanek, K. Z., & Berlind, P. 1999, *IAU Circ.* 7276
- Garnavich, P. M., & Quinn, J. 2000, *IAU Circ.* 7388
- Homan, J., Wijnands, R., & van der Klis, M. 1999, *IAU Circ.* 7121
- Hynes, R. I., Haswell, C. A., Norton, A. J., & Chaty, S. 1999, *IAU Circ.* 7294
- Kato, S., & Fukue, J. 1980, *PASJ*, 32, 377
- Leahy, D. A., Darbro, W., Elsner, R. F., Weisskopf, M. C., Sutherland, P. G., Kahn, S., & Grindlay, J. E. 1983, *ApJ*, 266, 160
- Markwardt, C. B., Marshall, F. E., & Swank, J. H. 1999, *IAU Circ.* 7274
- Markwardt, C. B., Focke, W. B., Swank, J. H., & Taam, R. E. 2000, *BAAS*, 195, 12603
- McCollough, M. L., & Wilson, C. A. 1999, *IAU Circ.* 7282
- Morgan, E. H., Remillard, R. A., & Greiner, J. 1997, *ApJ*, 482, 993
- Nowak, M. A., Wagoner, R. V., Begelman, M. C., & Lehr, D. E. 1997, *ApJ*, 477, L91
- Nowak, M. A., & Wagoner, R. V. 1992, *ApJ*, 393, 697
- Nowak, M. A., & Wagoner, R. V. 1993, *ApJ*, 418, 187
- Pooley, G. G., & Hjellming, R. M. 1999, *IAU Circ.* 7278
- Remillard, R. A., & Morgan, E. H. 2000, *BAAS*, 195, 3702
- Remillard, R. A., Morgan, E. H., McClintock, J. E., Bailyn, C. D., & Orosz, J. A. 1999a, *ApJ*, 522, 397

- Remillard, R. A., McClintock, J. E., Sobczak, G. J., Bailyn, C. D., Orosz, J. A., Morgan, E. H., & Levine, A. M. 1999b, *ApJ*, 517, L127
- Wagner, R. M., Smith, P. S., Schmidt, G. D., & Shrader, C. R. 1999, *IAU Circ.* 7279
- Wijnands, R., Homan, J., & van der Klis, M. 1999, *ApJ*, 526, L33
- Wood, A., Smith, D. A., Marshall, F. E., & Swank, J. 1999, *IAU Circ.* 7274
- Zhang, S. N., Cui, W., & Chen, W. 1997, *ApJ*, 482, L155

Table 1. PCA Observation Log¹

Obs.	Obs. Id.	Obs. Time (UT) ²	PCUs	Exp. (s)	CR (c/s)	HR
1	01-03	02:04:00–03:12:00	4	2640	3028	0.46
2	01-02	03:40:00–04:47:00	4	3060	3104	0.45
3	01-01	05:16:00–06:23:00	3	3480	2406	0.41
4	01-00	06:52:00–10:01:00	3	7440	2446	0.44

¹Columns: (1) designated observation number, (2) observation ID with prefix “40122–01–” omitted, (3) observation time interval, (4) number of PCUs on, (5) exposure time, (6) mean count rate per PCU, and (7) mean hardness ratio (the mean count rate of the 5.9–60 keV band divided by that of the 2–5.9 keV band).

²All observations were carried out on 18 October 1999.

Table 2. QPO Properties¹

Obs.	Low-Frequency QPO ²					High-Frequency QPO ³		
	Freq. (Hz)	FWHM (Hz)	RMS (%)	Peak Lag ⁴ (radian)	Cont. Lag ⁵ (radian)	Freq. (Hz)	FWHM (Hz)	RMS (%)
1	$5.97^{+0.01}_{-0.01}$	$0.44^{+0.02}_{-0.02}$	$7.38^{+0.09}_{-0.08}$	$0.31^{+0.04}_{-0.04}$	$-0.24^{+0.04}_{-0.04}$	187^{+14}_{-11}	95^{+46}_{-43}	$3.3^{+0.5}_{-0.7}$
	$2.92^{+0.08}_{-0.09}$	$0.40^{+0.18}_{-0.18}$	$0.8^{+0.1}_{-0.1}$					
	$11.74^{+0.05}_{-0.06}$	$2.1^{+0.2}_{-0.2}$	$3.12^{+0.10}_{-0.09}$					
2	$5.97^{+0.01}_{-0.01}$	$0.54^{+0.02}_{-0.02}$	$6.50^{+0.08}_{-0.08}$	$0.23^{+0.05}_{-0.05}$	$-0.24^{+0.06}_{-0.06}$	82^{+56}_{-26}	180^{+58}_{-37}	$3.8^{+0.3}_{-0.4}$
	$11.6^{+0.09}_{-0.09}$	$2.6^{+0.3}_{-0.3}$	$2.9^{+0.1}_{-0.1}$					
3	$7.3^{+0.3}_{-0.2}$	$5.8^{+1.0}_{-0.9}$	$3.3^{+0.3}_{-0.3}$	$-0.24^{+0.13}_{-0.13}$	$-0.26^{+0.12}_{-0.12}$
4	$5.95^{+0.01}_{-0.01}$	$0.57^{+0.02}_{-0.02}$	$5.31^{+0.06}_{-0.06}$	$0.24^{+0.04}_{-0.04}$	$-0.15^{+0.07}_{-0.07}$	150^{+17}_{-28}	124^{+53}_{-39}	$3.2^{+0.5}_{-0.6}$
	$10.9^{+0.2}_{-0.3}$	$4.5^{+0.7}_{-0.6}$	$2.9^{+0.2}_{-0.2}$					

¹The uncertainties shown represent roughly 1σ errors. Note that the fractional rms amplitudes are for the 5.9–60 keV band.

²Including (sub-)harmonics.

³For Obs. 2, the signal has very low Q, more like a broad “shoulder” than a QPO (see text).

⁴The peak lag is computed by averaging the measured phase lag over a frequency interval $(f_0 - w/5, f_0 + w/5)$, where f_0 is the centroid frequency of the QPO and w the width (FWHM).

⁵The continuum lag is computed by averaging the measure phase lag over (1, 10) Hz with $(f_0 - 5w, f_0 + 5w)$ excluded, except for Obs. 3 where the lag is averaged over (1, 15) Hz excluding $(f_0 - w, f_0 + w)$. Note that the difference between the peak lag and the continuum lag gives the phase lag associated with the QPO.

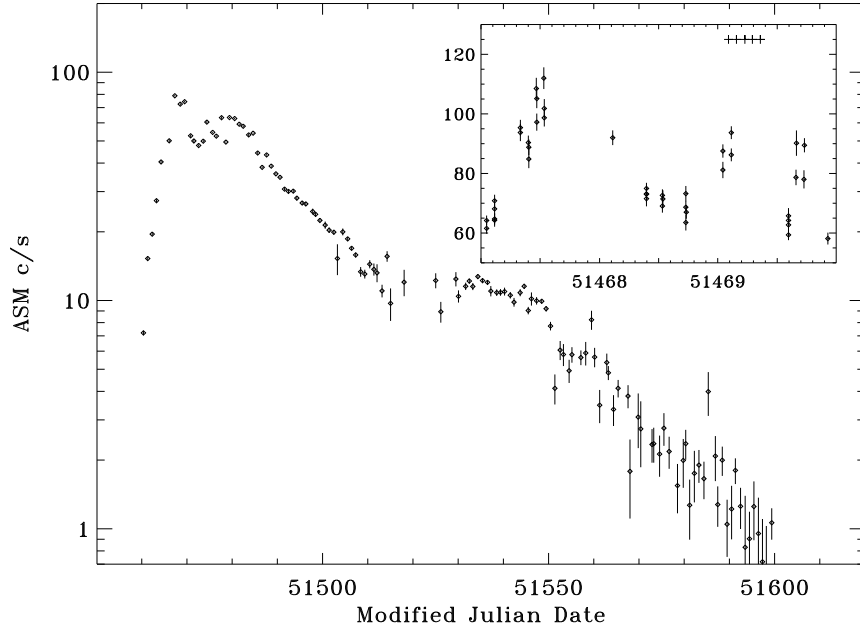


Fig. 1.— Daily-averaged ASM light curve of XTE J1859+226 during a recent X-ray outburst. The inset expands the light curve around the peak of the outburst when the PCA observations were carried out. Note that we chose to plot 90 dwell data in the inset for better coverage of the brief flares. Each cross marks the start time of a “good time interval” for each satellite orbit. For reference, MJD 51450 corresponds to 1999 September 29.

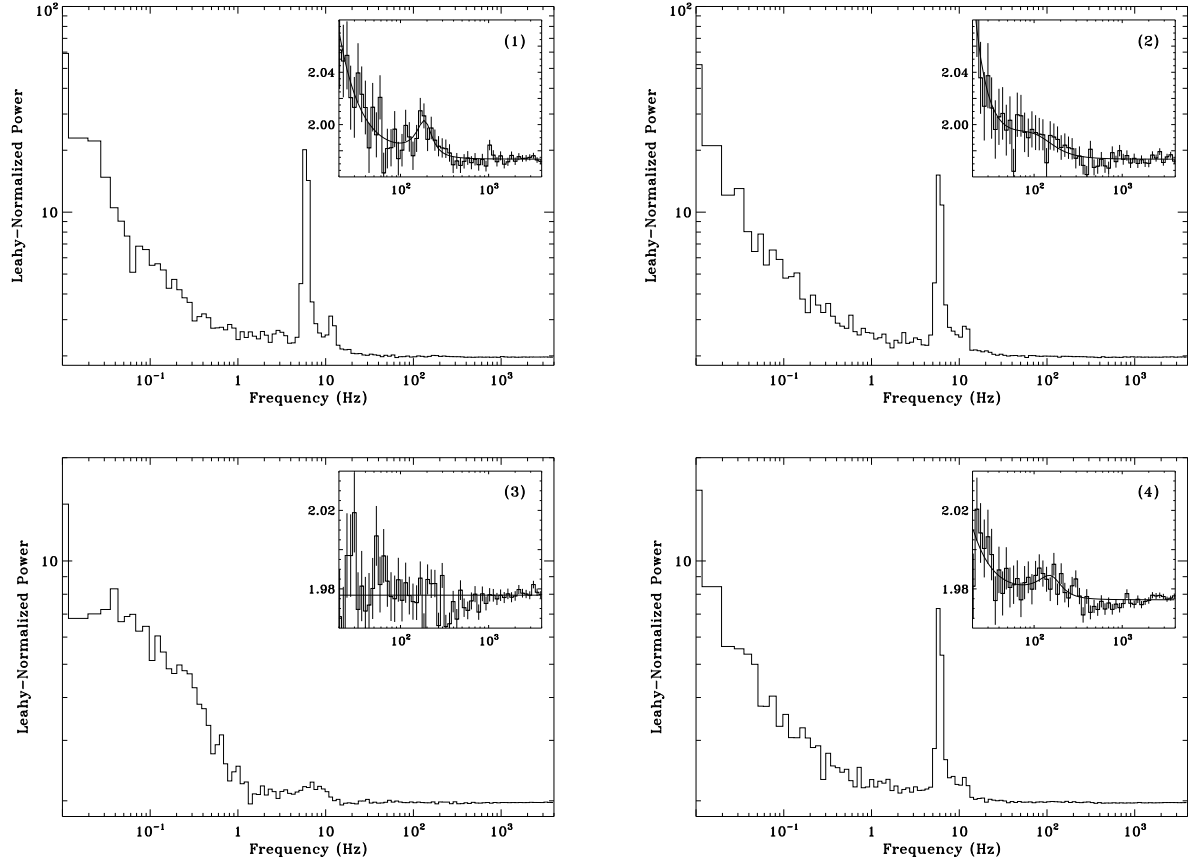


Fig. 2.— Power density spectra of XTE J1859+226. The insets provide an expanded view of the frequency range where the high-frequency QPOs are found. Note that the solid lines represent the best-fit to the data.

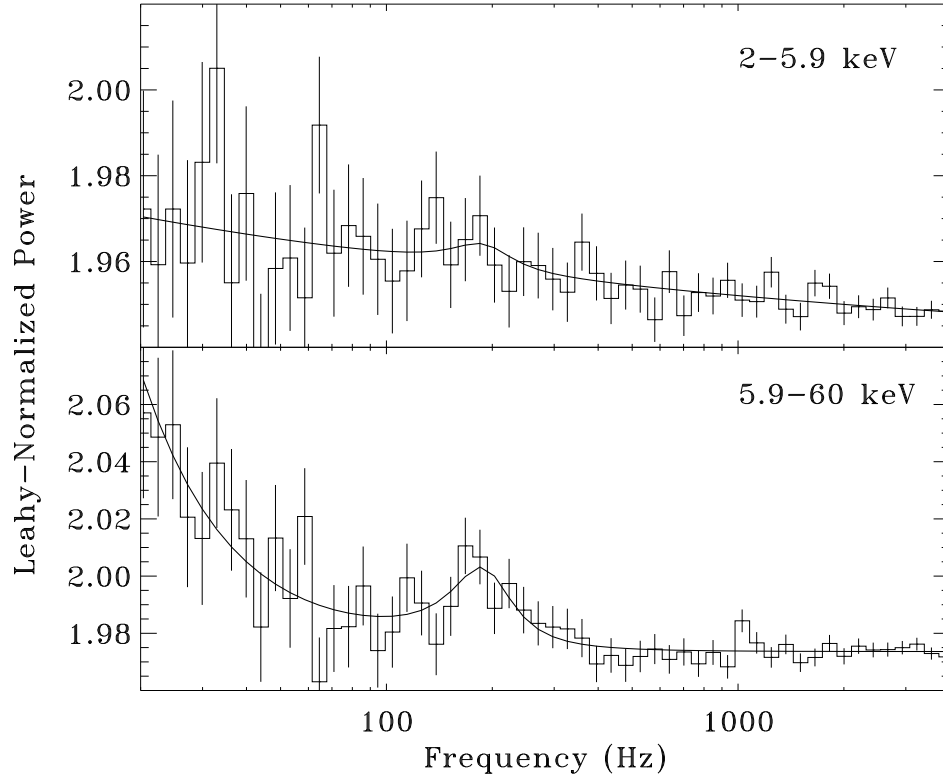


Fig. 3.— Power density spectra of XTE J1859+226 in two energy bands. These are made from observation 1, and zoom onto the frequency range where the high-frequency QPO is detected. The solid lines represent the best-fit model to the data, although for the soft band the frequency and width of the Lorentzian was fixed to those derived from the hard band (see text).